# Nuclear Magnetic Resonance Relaxation Study of Strychnine in Solution. Molecular Dynamics Models for the Interpretation of $^{13}C$ $T_1$ Data and Relaxation Mechanisms of the Quaternary Carbons

Hideaki FUJIWARA,* Yong-Zhong DA, Tatsuya TAKAGI, and Yoshio SASAKI

*Faculty of Pharmaceutical Sciences, Osaka University, 1–6 Yamadaoka, Suita, Osaka 565, Japan.* *Received March 6, 1989*

**Nuclear magnetic resonance relaxation times ($T_1$) of $^{13}C$ nuclei in strychnine have been measured in $CDCl_3$ at 2.35 T (25 MHz) to investigate the molecular dynamics and the structural information included in the relaxation times. The $T_1$ data of the proton-bearing carbons have been treated by a computer-aided method of analysis based on several models of molecular motion. The calculation supported an anisotropic nature of the molecular motion, although it is small. The $T_1$ data of quaternary carbons are discussed after estimating the dipole–dipole parts for these carbons: these parts are dependent on the number of α-protons attached to the adjacent atoms and amount to 50—60% of the total relaxation rates. Contributions of the relaxation mechanisms other than the dipole-dipole one are estimated for the quaternary carbons from the $T_1$ data including those at 11.74 T (125 MHz) reported elsewhere. Anisotropies in the chemical shift are also determined for the quaternary carbons. The anisotropy is relatively small for the carbonyl carbon attached to a nitrogen atom, indicating an electronegativity effect of the adjacent atom.**

**Keywords** strychnine; NMR $^{13}C$ relaxation time; relaxation mechanism; molecular dynamics; computer-aided analysis; chemical shift anisotropy; spectral assignment

Nuclear magnetic resonance (NMR) relaxation times include information on the molecular structure as well as the molecular dynamics. The relaxation times, however, have not been employed widely in the field of chemistry in contrast to the chemical shifts and coupling constants. This is probably due to experimental difficulties and problems of interpretation. Namely, the accuracy of experimental determination of relaxation times is low relative to that of chemical shifts and coupling constants. Also, although basic theories have been established,[1-4] practical applications of relaxation times require plenty of mathematical manipulations including molecular dynamics as well as geometrical data.[5] Recently, development of the pulse-Fourier transform method has greatly improved the accuracy of experimental relaxation times by enabling different modes of measurement and by enhancing the $S/N$ ratio. Recent development in computer technology also makes it possible to perform complex calculations that follow exactly the established relaxation theories.

In the present study, $^{13}C$ $T_1$ data were collected at 2.35 T (25 MHz) for a convulsant drug, strychnine (Chart 1). The data were analyzed based on several molecular dynamics models and are discussed together with the previous results[6] obtained at 11.74 T (125 MHz). The computer-aided analysis of $T_1$ data is shown to be fruitful for the derivation of chemical information from the relaxation times.

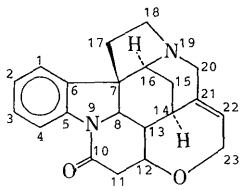

Chart 1. Strychnine

TABLE I. $^{13}C$ $T_1$ Analysis of Strychnine in $CDCl_3$ at 25 MHz[a]

| Shift (ppm) | Assignment | $T_{1,obsd}$ | $T^{DD}_{1,calcd}$[b] | | |
|---|---|---|---|---|---|
| | | | Model 1 | Model 2 | Model 3 |
| 169.1 | 10[c] | 18.7 ±0.9 | 36.3 | 36.2 | 35.6 |
| 142.2 | 5[c] | 28.3 ±1.1 | 67.3 | 63.4 | 61.6 |
| 140.4 | 21[c] | 13.2 ±0.6 | 17.5 | 17.6 | 17.2 |
| 132.7 | 6[c] | 23.2 ±1.0 | 48.7 | 48.7 | 47.3 |
| 128.4 | 3 | 1.40±0.06 | 1.57 | 1.43 | 1.41 |
| 127.1 | 22 | 1.47±0.04 | 1.53 | 1.48 | 1.45 |
| 124.2 | 2 | 1.53±0.03 | 1.57 | 1.58 | 1.53 |
| 122.3 | 1 | 1.50±0.05 | 1.61 | 1.63 | 1.54 |
| 116.2 | 4 | 1.50±0.05 | 1.62 | 1.61 | 1.55 |
| 77.7 | 12 | 1.51±0.05 | 1.53 | 1.51 | 1.54 |
| 64.6 | 23 | 0.86±0.02 | 0.81 | 0.83 | 0.84 |
| 60.3 | 8 | 1.55±0.04 | 1.59 | 1.61 | 1.62 |
| 60.3 | 16 | 1.55±0.04 | 1.55 | 1.59 | 1.53 |
| 52.7 | 20 | 0.80±0.03 | 0.81 | 0.80 | 0.80 |
| 52.2 | 7[c] | 19.2 ±0.8 | 21.9 | 22.4 | 22.1 |
| 50.6 | 18 | 0.83±0.02 | 0.80 | 0.82 | 0.79 |
| 48.4 | 13 | 1.50±0.04 | 1.54 | 1.52 | 1.52 |
| 43.0 | 17 | 0.80±0.02 | 0.81 | 0.83 | 0.82 |
| 42.6 | 11 | 0.88±0.05 | 0.82 | 0.84 | 0.84 |
| 31.7 | 14 | 1.59±0.05 | 1.53 | 1.55 | 1.58 |
| 27.1 | 15 | 0.78±0.05 | 0.80 | 0.76 | 0.75 |

*a*) The unit of $T_1$ is sec. *b*) Experimental data were fitted to several models of molecular reorientational motion excluding the data for *c*) quaternary carbons. Model 1: Isotropic model. Model 2: Axially symmetric model. Model 3: Fully anisotropic model.

## Experimental

Strychnine from Tokyo Kasei (above 98% pure) and $CDCl_3$ from Merck were used without further purification. The sample solution, 0.46 M in $CDCl_3$, was filled in a 10 mm o.d. tube with a vortex plug. It was first degassed by the conventional freeze-pump-thaw method, and then filled with Ar gas to suppress evaporation of the solvent.

The relaxation time was measured in an inversion-recovery mode with a JEOL PS-100 spectrometer at 25 MHz. The 90° pulse was 16 μs and the measuring temperature was 32 °C. Thirty-two FID's (free induction decays) were accumulated with a waiting time of 180 s. The measurement was repeated five times to obtain the averages and standard deviations of relaxation times.

The computer programs T1ANSOC[5,6] and MOLDYN[7] were used for the analysis of $T_1$ data. Calculations were done on NEAC S-1000 and SX-1 computers in the Computation Center, Osaka University.

## Results and Discussion

The $T_1$ values measured are listed in Table I including their standard deviations on repeated runs. The $T_1$ data were analyzed using the geometry of strychnine determined

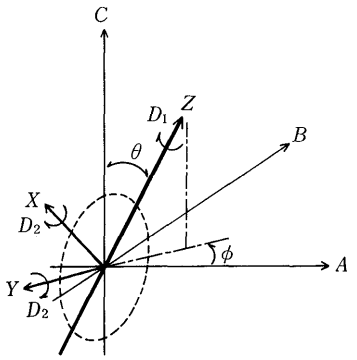


Fig. 1. Axially Symmetric Model: Relation between the Principal Axis System *XYZ* for the Molecular Motion and the Principal Axis System *ABC* for the Moment of Inertia

The inertial axes are taken as $I_A \geq I_B \geq I_C$, I being the moment of inertia. *Z* is the main (unique) axis for the motion. The *X* and *Y* axes are equivalent in the axially symmetric model and can be taken in any direction perpendicular to the *Z* axis. $D_1$ and $D_2$ mean the rate constants of the molecular reorientational motion.

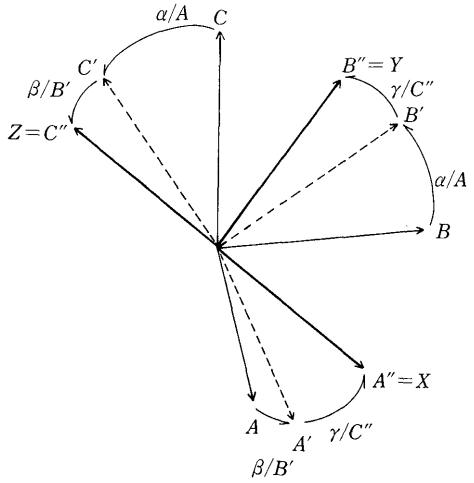


Fig. 2. Fully Anisotropic Model: Relation between the Principal Axis System *XYZ* for the Molecular Motion and the Principal Axis System *ABC* for the Moment of Inertia

The *ABC* axis system is rotated around *A* by an angle of α (obtaining *AB′C′*), around *B′* by an angle of β (*A′B′C″*), and around *C″* by an angle of γ (*A″B″C″*). The final axes of *A″*, *B″*, and *C″* are equal to *X*, *Y*, and *Z*, respectively. α/*A* means the rotation around the *A* axis.

in a crystal[8]: the locations of protons, however, were determined by calculation so that the C–H distances are all equal to a standard value, 1.09 Å, since the C–H distances cited from the crystal data include rather large scatterings which in turn induce very large uncertainties in the calculated relaxation times due to the sixth power dependence of the relaxation rate on the distance.

**Analysis of the $T_1$ Data of Proton-Bearing Carbons** The $T_1$ data of all proton-bearing carbons are assumed to be dominated by the dipole–dipole relaxation mechanism and were analyzed under the three models of molecular reorientational motion, isotropic, axially symmetric (Fig. 1), and fully anisotropic (Fig. 2) models. No internal motions are assumed since the molecule treated is composed of a rigid framework. Successful data fitting as described later supports this assumption.

The molecular dynamics parameters obtained at 25 MHz (for carbons) are listed in Table II together with the previous results obtained at 125 MHz.[6] The errors are

Table II. Molecular Dynamics Parameters of Strychnine in $CDCl_3$ Determined at 25 and 125 MHz

| Models | Parameters | 25 MHz | 125 MHz |
|---|---|---|---|
| Isotropic[a] | $D/10^9\,s^{-1}$ | 5.9±0.2 | 4.3±0.4 |
| | S.D./s | 0.070 | 0.111 |
| Axially symmetric[a] | $D_2/10^9\,s^{-1}$ | 5.3±0.2 | 3.3±0.2 |
| | $D_1/D_2$ | 1.3±0.1 | 1.9±0.3 |
| | θ | 17±45° | 11±28° |
| | φ | 3±9° | −12±79° |
| | S.D./s | 0.060 | 0.104 |
| Fully anisotropic[b] | $D_1/10^9\,s^{-1}$ | 7.1 | 6.6 |
| | $D_2/D_1$ | 1.2 | 1.7 |
| | $D_3/D_1$ | 1.5 | 2.7 |
| | α | 4° | −26° |
| | β | 4° | 8° |
| | γ | −26° | −29° |
| | S.D./s | 0.026 | 0.066 |

*a*) Calculated with the program "T1ANSOC". *b*) Calculated with the program "MOLDYN". This program does not afford error estimates for the parameters.

given for the parameters determined under the isotropic and axially symmetric models in Table II. These were estimated in the program T1ANSOC as 95% confidence ranges assuming independency between the variable parameters. It can be seen that θ and φ, which define the angles between the principal axes for the moment of inertia *ABC* and for the molecular reorientational motion *XYZ* (Fig. 1), are almost equal to zero when the error ranges are considered. This means that the two axis systems virtually coincide. Therefore, solvation is thought to be weak in the chloroform solution.

Among the three molecular dynamics models, the fully anisotropic model gives the smallest standard deviation (S.D.) between the observed and recalculated relaxation times. However, when compared with similar plots at 125 MHz,[6] the superiority of the anisotropic models is not so clear in Fig. 3. Here, standard deviation is adopted as a measure of fit instead of the root-mean-square deviation, considering the different numbers of adjustable parameters in the three models. In the present case, the $T_1$ data of proton-bearing carbons are separated rather clearly into the two groups of CH and $CH_2$ carbons. The authors suggest that the small site dependency of the $T_1$ data was masked by the inferior long-term stability of the electro-magnet compared to the superconducting one and the longer waiting time adopted in the present case. In fact, the ratio of the molecular reorientational rate constant *D* is decreased toward unity in the present case (Table II). However, the molecular dynamics parameters including their error estimates support an anisotropic motion of the strychnine molecule.

**Analysis of the $T_1$ Data of the Quaternary Carbons** Since molecular dynamics parameters are obtained above from the $T_1$ data of proton-bearing carbons, the dipole–dipole part $T_1^{DD}$ of quaternary carbons can be calculated using these parameters together with the geometric parameters. Also, the contribution from mechanisms other than the dipole–dipole one, $T_1^{others}$, can be calculated according to the equation:

$$1/T_{1,calcd}^{others} = 1/T_{1,obsd} - 1/T_{1,calcd}^{DD} \quad (1)$$

Then, the contribution of dipole–dipole relaxation is calcu-

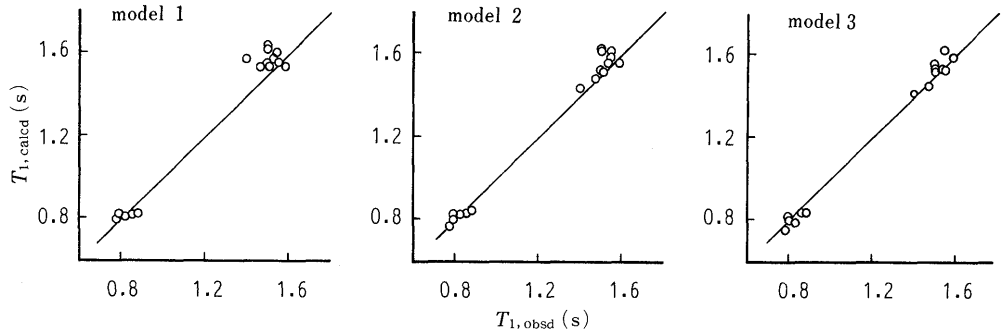


Fig. 3. Correlation between the Calculated and Observed $T_1$ Values for the Three Models of Molecular Motion

Model 1: Isotropic model ($r=0.988$). Model 2: Axially symmetric model ($r=0.993$). Model 3: Fully anisotropic model ($r=0.997$). The correlation coefficient $r$ between the observed and the calculated $T_1$ values is denoted in parentheses.

TABLE III. $^{13}C$ $T_1$ Analysis of Quaternary Carbons in Strychnine at 25 and 125 MHz[a]

| Shift / ppm | Assignment | $T_{1,\mathrm{obsd}}$ | $T^{\mathrm{DD}}_{1,\mathrm{calcd}}$ | $T_1^{\mathrm{others}}$ | $T_{1,\mathrm{obsd}}/T^{\mathrm{DD}}_{1,\mathrm{calcd}}$ | Type of carbon | Number of α-protons |
|---|---|---|---|---|---|---|---|
| 169.1 | 10 | 18.71 | 35.60 | 39.44 | 0.53 | $sp^2$ | 2 |
| | | (8.58) | (26.14) | (12.78) | (0.33) | | |
| 142.2 | 5 | 28.25 | 61.60 | 52.18 | 0.46 | $sp^2$ | 1 |
| | | (8.02) | (43.37) | (9.84) | (0.18) | | |
| 140.4 | 21 | 13.23 | 17.20 | 57.32 | 0.77 | $sp^2$ | 4 |
| | | (4.38) | (13.07) | (6.59) | (0.34) | | |
| 132.7 | 6 | 23.21 | 47.30 | 45.57 | 0.49 | $sp^2$ | 1 |
| | | (7.91) | (35.73) | (10.16) | (0.22) | | |
| 52.2 | 7 | 19.24 | 22.10 | 148.7 | 0.87 | $sp^3$ | 4 |
| | | (13.08) | (16.90) | (57.86) | (0.77) | | |

a) The unit of $T_1$ is s. Values in parentheses are the data at 125 MHz.[6] Values estimated according to the fully anisotropic model are cited for $T^{\mathrm{DD}}_{1,\mathrm{calcd}}$.

lated as the ratio in the relaxation rates $(1/T^{\mathrm{DD}}_{1,\mathrm{calcd}})/(1/T_{1,\mathrm{obsd}})$, *i.e.*, $T_{1,\mathrm{obsd}}/T^{\mathrm{DD}}_{1,\mathrm{calcd}}$. These are also listed in Table III. The ratio of $T_{1,\mathrm{obsd}}/T^{\mathrm{DD}}_{1,\mathrm{calcd}}$ is increased for the carbons having a larger number of α-protons and is decreased at higher magnetic field, and it is high for the saturated $sp^3$ carbons compared to that for the unsaturated $sp^2$ carbons. The $^{13}C$ $T_1$ values of quaternary carbons were reported to be dominated usually by the dipole–dipole mechanism when observed at the lower fields attainable by commercial electro- or permanent magnets.[8] A method of assignment was proposed for the quaternary carbons based on the $T_1$ values.[8] However, the part of the dipole–dipole relaxation expressed by the ratio mentioned above is as small as 50% at 25 MHz for the carbons having one or two α-protons (Table III). Therefore, for a wider application of the proposed method of analysis, it seems necessary to take into account the contribution of mechanisms other than the dipole–dipole one, even if fortunately in the present case $T_{1,\mathrm{obsd}}$ parallels $T^{\mathrm{DD}}_{1,\mathrm{calcd}}$ for the $sp^2$ carbons at 25 MHz, reflecting roughly the number of α-protons.

**Separation of $T_1^{\mathrm{others}}$ into Two Components for the Quaternary Carbons: Use of an Iterative Method** As mechanisms other than the dipole–dipole one, we may consider chemical-shift-anisotropy ($T_1^{\mathrm{CA}}$), spin-rotation interaction ($T_1^{\mathrm{SR}}$), and scalar-coupling ($T_1^{\mathrm{SC}}$).[1,2] The last one $T_1^{\mathrm{SC}}$ becomes nontrivial for quaternary halogen-bearing carbons[2] and is not considered here. The following equation holds for the present case:

$$1/T_1^{\mathrm{others}}=1/T_1^{\mathrm{CA}}+1/T_1^{\mathrm{SR}} \tag{2}$$

$T_1^{\mathrm{CA}}$ and $T_1^{\mathrm{SR}}$ can be expressed as follows[2]:

$$\frac{1}{T_1^{\mathrm{CA}}}=\frac{2}{15}(2\pi\nu_0)^2(\sigma_{\parallel}-\sigma_{\perp})^2\cdot\frac{\tau_c}{1+(2\pi\nu_0)^2\cdot\tau_c^2} \tag{3}$$

$$\frac{1}{T_1^{\mathrm{SR}}}=\left(\frac{2\pi IkT}{h^2}\right)\left(\frac{C_{\parallel}^2+2C_{\perp}^2}{3}\right)\cdot\tau_J \tag{4}$$

where molecular motion is assumed to be isotropic for simplicity and the correlation time $\tau_c$ is related to the rate constant $D$ adopted above by $\tau_c=1/6D$. In the above equations, $\nu_0$ is the NMR frequency, $\sigma_{\parallel}$ and $\sigma_{\perp}$ are the components of chemical shielding tensor, $I$ is the moment of inertia of the molecule, $C_{\parallel}$ and $C_{\perp}$ are the components of the spin-rotation tensor, $\tau_J$ is the angular momentum correlation time, and other symbols have the conventional meanings. Since the extreme narrowing condition holds for the present case as may be seen from the result of calculation above, Eq. 3 is modified as follows,

$$1/T_1^{\mathrm{CA}}=(2/15)(2\pi\nu_0)^2(\Delta\sigma)^2\tau_c \tag{5}$$

where $\Delta\sigma$ is $\sigma_{\parallel}-\sigma_{\perp}$. Also Eq. 4 is modified as follows, considering the relation $\tau_c\tau_J=I/6kT$.[2]

$$1/T_1^{\mathrm{SR}}=(\pi I^2/3h^2)\{(C_{\parallel}^2+2C_{\perp}^2)/3\}(1/\tau_c) \tag{6}$$

Therefore, it is seen that $T_1^{\mathrm{CA}}$ is inversely proportional to $\tau_c$ and $\nu_0^2$ whereas $T_1^{\mathrm{SR}}$ is proportional to $\tau_c$. By making use of such differences in $T_1^{\mathrm{CA}}$ and $T_1^{\mathrm{SR}}$, $T_1^{\mathrm{others}}$ can be separated into the two components from the $T_1$ data measured at two different magnetic fields. $T_1^{\mathrm{others}}$ is expressed as follows at two different NMR frequencies, 125 and 25 MHz.

$$1/T_1^{\text{others}(125)} = 1/T_1^{\text{CA}(125)} + 1/T_1^{\text{SR}(125)} \quad (7)$$

$$1/T_1^{\text{others}(25)} = 1/T_1^{\text{CA}(25)} + 1/T_1^{\text{SR}(25)} \quad (8)$$

To take into account a small discrepancy in the $\tau_c$ values determined above at 125 and 25 MHz, two correlation times, $\tau_c^{(125)}$ and $\tau_c^{(25)}$, are introduced. Such a small discrepancy may be brought about by a small difference in the temperature of NMR measurement, even if the same sample is used for th measurement. Under these conditions, the following equations hold for $T_1^{\text{CA}}$ and $T_1^{\text{SR}}$ of each carbon measured at the two frequencies:

$$T_1^{\text{CA}(25)}/T_1^{\text{CA}(125)} = 25\cdot\tau_c^{(125)}/\tau_c^{(25)}, \text{ and hence}$$

$$1/T_1^{\text{CA}(25)} = \{\tau_c^{(25)}/25\tau_c^{(125)}\}\{1/T_1^{\text{CA}(125)}\} \quad (9)$$

$$T_1^{\text{SR}(25)}/T_1^{\text{SR}(125)} = \tau_c^{(25)}/\tau_c^{(125)}, \text{ and hence}$$

$$1/T_1^{\text{SR}(25)} = \{\tau_c^{(125)}/\tau_c^{(25)}\}\{1/T_1^{\text{SR}(125)}\} \quad (10)$$

From Eqs. 7 to 10,

$$\frac{1}{T_1^{\text{others}(125)}} - \frac{1}{T_1^{\text{others}(25)}} = \frac{1}{T_1^{\text{CA}(125)}}\left\{1-\left(\frac{1}{25}\frac{\tau_c^{(25)}}{\tau_c^{(125)}}\right)\right\} + \frac{1}{T_1^{\text{SR}(125)}}\left\{1-\frac{\tau_c^{(125)}}{\tau_c^{(25)}}\right\} \quad (11)$$

is obtained. Therefore, if $\tau_c^{(125)}$ is exactly equal to $\tau_c^{(25)}$, the term $T_1^{\text{SR}(125)}$ drops out of Eq. 11 and $T_1^{\text{CA}(125)}$ is obtained from the values of $T_1^{\text{others}}$ at 125 and 25 MHz. But this is not the case, and hence an iterative method must be adopted.

First, $\tau_c^{(125)}$ is assumed to be equal to $\tau_c^{(25)}$, and $T_1^{\text{CA}(125)}$ is obtained, neglecting the term of $T_1^{\text{SR}(125)}$ in Eq. 11:

$$1/[T_1^{\text{CA}(125)}]_0 = \{1/T_1^{\text{others}(125)} - 1/T_1^{\text{others}(25)}\}/\{1-(\tau_c^{(25)}/25\tau_c^{(125)})\} \quad (12)$$

Here, $[\ ]_0$ is used to denote an initial estimate. Then, an initial estimate of $T_1^{\text{SR}(125)}$, $[T_1^{\text{SR}(125)}]_0$, is obtained by using Eq. 7.

Second, the first iterated value of $T_1^{\text{CA}(125)}$, *i.e.*, $[T_1^{\text{CA}(125)}]_1$, is obtained from the value of $[T_1^{\text{SR}(125)}]_0$ by using the following equation with $n=1$ which is a version of Eq. 11.

$$\frac{1}{[T_1^{\text{CA}(125)}]_n} = \left\{\left(\frac{1}{T_1^{\text{others}(125)}} - \frac{1}{T_1^{\text{others}(25)}}\right) - \frac{1}{[T_1^{\text{SR}(125)}]_{n-1}}\left(1-\frac{\tau_c^{(125)}}{\tau_c^{(25)}}\right)\right\} \Big/ \left\{1-\left(\frac{\tau_c^{(25)}}{25\tau_c^{(125)}}\right)\right\}$$

$$= \frac{1}{[T_1^{\text{CA}(125)}]_0} - \frac{1}{[T_1^{\text{SR}(125)}]_{n-1}}\left(1-\frac{\tau_c^{(125)}}{\tau_c^{(25)}}\right) \Big/ \left\{1-\left(\frac{\tau_c^{(25)}}{25\tau_c^{(125)}}\right)\right\} \quad (13)$$

$[T_1^{\text{SR}(125)}]_1$ is then determined according to Eq. 7.

The second step is repeated until $[T_1^{\text{CA}(125)}]_n$, and hence $[T_1^{\text{SR}(125)}]_n$, become independent of $n$. In the present study, five steps until $n=5$ were sufficient to obtain virtually constant values of the two components. The results are summarized in Table IV. It can be seen that the spin-rotation mechanism and the chemical-shift-anisotropy one are less effective for $sp^3$ carbon. This result is in accordance with the suggested parallel relation between $1/T_1^{\text{CA}}$ and $1/T_1^{\text{SR}}$.[9]

**Determination of the Chemical-Shift-Anisotropy $\Delta\sigma$ for the Quaternary Carbons** By the use of Eq. 5 together with the experimental values obtained above, $\Delta\sigma$ can be estimated:

Table IV. Separation of $T_1^{\text{others}}$ into the Two Components $T_1^{\text{CA}}$ and $T_1^{\text{SR}}$ and the Chemical Shift Anisotropies $\Delta\sigma$ in Strychnine[a]

| Shift / ppm | Assignment | $T_{1,\text{calcd}}^{\text{DD}}$ (Model 1) | $T_1^{\text{others}}$ | $T_1^{\text{CA}}$ | $T_1^{\text{SR}}$ | $\Delta\sigma$ / ppm |
|---|---|---|---|---|---|---|
| 169.1 | 10 | 36.3 | 38.6 | 558.6 | 41.7 | |
| | | (26.6) | (12.7) | (16.4) | (56.5) | (138.7) |
| 142.2 | 5 | 67.3 | 48.8 | 374.4 | 56.1 | |
| | | (49.4) | (9.60) | (11.0) | (76.6) | (169.4) |
| 140.2 | 21 | 17.5 | 53.7 | 246.2 | 68.7 | |
| | | (12.8) | (6.70) | (7.22) | (93.8) | (208.9) |
| 132.7 | 6 | 48.7 | 44.3 | 409.5 | 49.7 | |
| | | (35.7) | (10.2) | (12.0) | (67.6) | (161.9) |
| 52.2 | 7 | 21.9 | 155.7 | 3567 | 162.8 | |
| | | (16.0) | (71.1) | (104.6) | (221.9) | (54.9) |

a) Values in parentheses are the data at 125 MHz. The unit of $T_1$ is s. $T_1^{\text{others}}$ is obtained by using the $T_{1,\text{calcd}}^{\text{DD}}$ estimated according to the isotropic model.

$$\frac{\Delta\sigma}{\text{ppm}} = \pm\left\{\frac{1}{T_1^{\text{CA}(125)}}\frac{15}{2}\frac{1}{\tau_c^{(125)}}\right\}^{1/2}\cdot\frac{1}{2\pi\cdot 125} \quad (14)$$

These values are listed in Table IV, where the positive sign is taken in the above equation. In Table IV, $T_{1,\text{calcd}}^{\text{DD}}$ estimated according to the isotropic model is adopted, since Eq. 5 has been derived based on this model and includes the isotropic correlation time $\tau_c$. When $T_{1,\text{calcd}}^{\text{DD}}$ estimated according to the fully anisotropic model is cited, $\Delta\sigma$ changes by amounts of *ca.* 1 ppm for the $sp^2$ carbons and of 10 ppm for the $sp^3$ carbon. The values of $\Delta\sigma$ have been collected for a limited number of compounds.[10,11] The values obtained in the present study are consistent with the reported values of other compounds. The value for carbon-10 might be a little small compared to the available values of carbonyl carbons. However, $\Delta\sigma$ changes rather widely depending on the electronic state of the C=O bond, and this value is especially decreased when an electronegative atom is attached to the C=O bond, as in the case of the –COO– group.[10,11] Therefore, the value of $\Delta\sigma$ for the carbon-10 is thought to be reasonable. In this regard, $^{13}C$ $T_1$ analysis as described here may become a useful tool for the assignment of quaternary carbons through the estimation of $\Delta\sigma$, although such a method of assignment has not been proposed yet. The available data of $\Delta\sigma$ are limited in number,[10,11] and further detailed discussion must await accumulation of many more $\Delta\sigma$ values.

**Discussion of the Nuclear Overhauser Effect (NOE) Factors** The NOE factor can be calculated from Eq. 15,

$$\eta/\eta_{\max} = T_1/T_1^{\text{DD}} \quad (15)$$

where $\eta_{\max}$ is equal to $\gamma_s/2\gamma_I$, *i.e.*, 1.987, for a C–H pair. This value is also included in Table III for the quaternary carbons. For the proton-bearing carbons, this factor was assumed to be maximum. In Table IV, $T_1^{\text{others}}$ is shown to amount to 40—150 s for the quaternary carbons, and hence similar values are expected for the proton-bearing carbons as well. The $T_{1,\text{obsd}}$ values lie between 0.8 and 1.6 s for the proton-bearing carbons, and hence the values of $\eta$ are estimated to be larger than 1.91 for these carbons. In this case, the difference in $T_{1,\text{obsd}}$ and $T_{1,\text{calcd}}^{\text{DD}}$ is roughly 0.05 s and comparable to experimental error. In this stage of our calculation, it became possible to repeat a similar analysis of the $T_1$ data of the proton-bearing carbons without

assuming maximum NOE factors. That is, the contribution of $T_1^{CA}$ at least can be subtracted from the $T_{1,obsd}$ data by estimating the $T_1^{CA}$ values according to Eq. 5 together with the $\tau_c$ values reached above and the available standard values for $\Delta\sigma$. Such a correction will be of significance at a higher magnetic field, since the contribution of $T_1^{CA}$ is increased proportionally to the square of the NMR frequency. When the $sp^2$ carbons are considered, for which $T_1^{CA}$ is a larger contributor than for the $sp^3$ carbons, the difference between the values of $T_{1,obsd}$ and $T_{1,calcd}^{DD}$ is around 0.15 s. Such a difference is small but may not be neglected. However, since the number of $sp^2$ carbons included in the simulation of the $T_1$ data is small compared to the total number of carbons used for the calculation, *i.e.*, 5 among 16, the calculation is expected to be virtually unchanged if the $T_1^{CA}$ term is allowed for. Also, the contribution of the $T_1^{SR}$ term is very small. Therefore, no futher attempt was made to correct the observed $T_1$ data for the proton-bearing carbons.

In conclusion, quantitative treatment of the $T_1$ data by means of a computer-aided method of analysis has given informations on the dynamic dehavior of strychnine in solution and on the chemical shift anisotropies of the quaternary carbons, showing that such a method of analysis will be of importance for the spectral assignment and for the determination of chemical structures as well as for studies on the dynamic behavior in solution.

**Acknowledgement** The authors are grateful to Dr. Masami Sawada and Yoshio Takai of the Institute of Industrial Sciences, Osaka University for the NMR facilities.

**References**

1) A. Abragam, "The Principles of Nuclear Magnetism," Oxford University Press, Oxford, 1961.
2) T. C. Farrar and E. D. Becker, "Pulse and Fourier Transform NMR," Academic, New York, 1971.
3) D. E. Woessnor, *J. Chem. Phys.*, **37**, 647 (1962).
4) H. Shimizu, *J. Chem. Phys.*, **37**, 765 (1962).
5) H. Fujiwara, T. Takagi, M. Sugiura, and Y. Sasaki, *J. Chem. Soc., Perkin Trans. 2*, **1983**, 903.
6) H. Fujiwara, M. Watanabe, Y. Da, D. Zheng, and Y. Sasaki, *Anal. Sci.*, in press.
7) A. Kumar, D. J. Craik, and G. C. Levy, QCPE Program No. 489, Indiana University, 1983.
8) *a*) F. W. Wehrli, *J. Chem. Soc., Chem. Commun.*, **1973**, 379; *b*) *Idem, Adv. Mol. Relax. Process*, **6**, 139 (1974); *c*) *Idem*, "Topics in Carbon-13 NMR Spectroscopy," Vol. 3, ed. by G. C. Levy, John Wiley, New York, 1976, Chap. 6.
9) Ref. 2, p. 65.
10) B. R. Appleman and B. P. Dailey, in "Advances in Magnetic Resonance," Vol. 7, ed. by J. S. Waugh, Academic, New York, 1974, p. 231.
11) M. Mehring, "High Resolution NMR Spectroscopy in Solids," Springer, Berlin, 1976.